行政院國家科學委員會專題研究計畫　期中進度報告

藍/紫光發光元件磊晶及製程之研究(1/3)

計畫類別：個別型計畫
計畫編號：NSC94-2215-E-009-082-
執行期間：94 年 08 月 01 日至 95 年 07 月 31 日
執行單位：國立交通大學光電工程學系(所)

計畫主持人：王興宗

計畫參與人員：王興宗教授，盧廷昌助理教授，黃根生博士，凌碩均等共 6 位碩士生

報告類型：精簡報告

處理方式：本計畫可公開查詢

中　華　民　國 95 年 5 月 29 日

行政院國家科學委員會補助專題研究計畫 □ 成 果 報 告
■期中進度報告

藍紫光發光元件磊晶及製程之研究(1/3)

計畫類別：■ 個別型計畫　　□ 整合型計畫
計畫編號：NSC　94－2215－E－009－082－
執行期間：94 年 06 月 01 日至 97 年 05 月 31 日

計畫主持人：　王興宗 教授
共同主持人：
計畫參與人員：盧廷昌、黃根生

成果報告類型(依經費核定清單規定繳交)：■精簡報告　□完整報告

本成果報告包括以下應繳交之附件：
□赴國外出差或研習心得報告一份
□赴大陸地區出差或研習心得報告一份
□出席國際學術會議心得報告及發表之論文各一份
□國際合作研究計畫國外研究報告書一份

處理方式：除產學合作研究計畫、提升產業技術及人才培育研究計畫、列管計畫及下列情形者外，得立即公開查詢
□涉及專利或其他智慧財產權，□一年□二年後可公開查詢

執行單位：國立交通大學光電工程研究所

中　華　民　國　九十五　年　五　月　二十四　日

中文摘要

關鍵字:氮化鋁鎵, 傅氏變換紅外光譜, 氮化鎵銦/氮化鋁鎵多層量子井, 紫外光發光二極體.

利用有機金屬氣相磊晶系統成長不同鋁成分氮化鋁鎵薄膜。x 光繞射儀和傅氏變換紅外光譜分析其高質量的磊晶品質。光學聲子 A_1(TO), E_1(TO), A_1(LO) 和 E_1(LO)的頻率隨鋁成分而改變。A_1（TO）和 A_1（LO）光學聲子呈現單模並有良好的對稱性，窄的線寬以及對鋁成分的大的線型變化。A_1（TO）和 A_1（LO）光學聲子隨鋁成分線型變化的斜率分別為 69 和 84 cm^{-1}。這些光學聲子將是決定氮化鋁鎵的鋁成分和結構的最好的參數。利用氮化鋁鎵作為位能障來提高載流子的局限和減少自吸收。引入一種新的磊晶程序成長氮化鎵銦的井。從光致發光光譜來看，在 380nm 左右有很強的發光峰。紫外光發光二極體製程初步結果顯示良好的內部量子效率

English Abstract

Keyword: AlGaN, FTIR, InGaN/AlGaN multiple quantum well, UVLED.

High quality $Al_xGa_{1-x}N$ (0<x<1) alloys grown by MOCVD were studied by using X-ray diffraction and Fourier transform infrared reflectance (FTIR) measurements. The Al compositional dependence of phonons having A_1 (TO), E_1 (TO), A_1 (LO) and E_1 (LO) symmetry was determined. The A_1 (TO) and A_1 (LO) modes, displayed a one-mode behavior and had a well defined symmetry, small linewidth and a large linear dependence of the phonon frequency upon alloy composition. The A_1 (TO) and A_1 (LO) modes linearly increased with Al composition by the large slopes of 69 and 84 cm^{-1}, respectively. These phonons modes shall be the best candidates for the compositional and structural characterization of AlGaN alloys. AlGaN as barrier layer was used to increase the carrier confinement and reduce self-absorption effect. The novel multi-step growth process was introduced to grow InGaN well layers. From photoluminescence measurement of the samples, strong UV emission peak around 380 nm can be observed. The UV-LEDs devices also were processed and the preliminary characterization of electroluminescence was shown good internal quantum efficiency.

INTRODUCTION

The high emission efficiency GaN-based light-emitting diodes (LEDs) have been applied between the ultraviolet (UV) and amber spectral regions.[1–6] Recently, UV LEDs have been strongly desired for several applications such as a light source for exciting phosphor, medical equipment, an air cleaner and an environmental sensor. In particular, it is important to fabricate white LEDs by coupling UV LEDs and phosphors.[7] White LEDs have been in high demand for the solid state lighting technology and the most challenging application for white LEDs is as a replacement of conventional incandescent and fluorescent lamp. However most of the phosphors for white fluorescent lamps have the high down-conversion quantum efficiency of less than 380 nm UV spectral region. Therefore, it is very important to develop high-efficiency UV LEDs that emit about 380 nm light in order to fabricate high luminous efficacy and high average color rendering white LEDs. Several groups reported that the quantum efficiency of UV LEDs is sensitive to the threading dislocation density (TDD)[8, 9] and is improved by growing nitride films on low TDD substrates such as GaN substrates. [10, 11] However, the external quantum efficiency (η_{ex}) of the reported UV LEDs is only a few %.[8–13] The reason for this low η_{ex} is mainly thought to be that UV light is absorbed in the thick GaN contact layer under the active layer. It was reported that the crystal quality of the AlGaN layer grown on the high crystal quality GaN layer is higher than that of the AlGaN grown directly on a sapphire substrate.[8] The UVLEDs require high quality p-type and n-type AlGaN on both sides of the active region to form heterojunction; However, the efficiency is very low for the UVLEDs, the high quality AlGaN can improve the output power and emission spectrum. In addition, it is necessary to improve the efficiency by replacing barrier layer material GaN with AlGaN, introducing quaternary InAlGaN-based system, or optimizing the device structure to enhance carrier confinement in active layer and increase injection current density. [14-16] Recently, Kwon et al. proposed ultra thin indium rich InGaN/GaN MQWs which exhibited strong near ultraviolet emission.[17] According to TEM and PL observations, the huge confinement of carrier by the high quality and ultra thin InGaN with abrupt interface cause strong UV emission.

In this report, the higher quality AlGaN epilayer grown by MOCVD were characterized by x-ray diffraction and photoluminescence and Fourier transforms infrared reflectance. The results show high quality AlGaN epilayer. The AlGaN epilayer as barrier layer to increase the carrier confinement and reduce self-absorption effect were studied. The multi-step growth process was introduced to grow InGaN well layers. From photoluminescence measurement of the samples, strong UV emission peak around 380 nm can be observed. The UV-LEDs also were processed and the preliminary characterization of electroluminescence was shown below.

EXPERIMENTS

The AlGaN epilayers and whole UVLED wafer structure was grown by the metal-organic chemical vapor deposition (MOCVD) system (EMCORE D-75) on the polished optical-grade C-face (0001) 2” diameter sapphire substrate. The sapphire substrate was placed on a graphite susceptor with a filament heater of the vertical type reactor. Trimthylgallium (TMGa), Trimthylaluminum (TMAl), and ammonia (NH_3) were used as the Ga, Al and N sources,

respectively. For AlGaN epilayers, a normal 30-nm-thick GaN nucleation layer was deposited at 530 ^{o}C. Before growing a 0.4-μm-thick $Al_xGa_{1-x}N$ film, a 2-μm-thick GaN buffer layer was grown on the substrate. All the growth conditions of GaN buffer layers were the same. For x of $Al_xGa_{1-x}N$ was less than 0.3, the samples were grown in N_2 and H_2 mixture ambient gas and at pressure of 100 Torr. For $0.3 < x < 1$, the samples were grown in N_2 and H_2 mixture ambient gas and at pressure of 50 Torr for a better Al incorporation efficiency.[18] For the AlN layer, in order to obtain better crystal quality, the samples were grown in a pure N_2 ambient gas and at pressure of 100 Torr. For the whole UVLED structure, n-type GaN layer was grown under InGaN/AlGaN MQW active layer in UVLED epitaxial structure. Then p-type GaN layer was grown on the active layers. After epitaxial growth, The compositions and crystal quality of $Al_xGa_{1-x}N$ films on GaN were measured by using a double crystal X-ray diffraction (Bede Scientific D1). The infrared reflectivity spectra were collected at room temperature by Bomen Fourier transform infrared spectrometer. We used nonpolarized light and a Fourier transform spectrometer, equipped with KBr beam splitter and a mercurcy-cadmium-tellride detector cooled down to 77K. We worked at incident angle of 75^{o} (Brewster's angle was about 68^{o}). The sample size should be lager than 1.5×1.5 cm^2 to collect the all reflected beams. The UVLED devices were measured by photoluminescence (PL) system using the He-Cd laser as the excitation source. By fabricating the UVLED device, the mesa region of the device was etching by inductivity coupled plasma (ICP) dry etching process by using the Cl_2 gas to define the n-type and p-type GaN region. Then the SiO_2 layer was deposited on the mesa region with a 20 μm open aperture region as the current confined layer. The thin Ni/Au (with 50Å/50Å-thick) was deposited on the open aperture region for the current spreading issue. Then the Ti/Al and Ni/Au metal were deposited as the n-type and p-type metal. The emission property of UVLEDs were compared in this experiment. And the EL emission spectrum and the related optical output power of the Sample A and Sample B were measured by the optical spectrum analyzer (OSA) system. A scanning near-field optical microscopy (Alpha-SNOM) was used to analyze the micro-optical property of the UVLED devices. The EL emission images were also observed by the optical microscopy (OM).

RESULTS AND DISCUSSION

Fig.1 shows the double crystal x-ray diffraction rocking curve (0004) of $Al_xGa_{1-x}N$ samples. The Al composition can be calculated from the diffraction angle separation between AlGaN and GaN peaks. The FWHM of (0004) diffraction peak of $Al_xGa_{1-x}N$ film increases when the Al composition increases from 0.1 to 0.4. The incorporation rate increases continuously, as the flow rate of TMA becomes higher. The quality of $Al_xGa_{1-x}N$ film becomes worse when the flow rate of TMA becomes higher. The FWHM of $Al_xGa_{1-x}N$ film decreases when the Al composition increases further. Because lower growth process of 50 torr was used to grow $Al_xGa_{1-x}N$ ($0.4 < x < 1$) film, the aluminum incorporation increases and the quality of film also was improved. Pure nitrogen as a carrier gas was used to grow AlN film. The narrow FWHM about 270 arcsec of x-ray diffraction peaks shows high quality of AlN film.

Fig. 2 shows the variation of the different aluminum composition $Al_xGa_{1-x}N$ alloys with $0 < x \leq 1$. The solid line β connected dips at wavenumber of 758 cm^{-1}, was attributed to the GaN-like A_1

(LO) modes emitted from the underneath GaN buffer layer. Similarly, the solid line γ corresponded to the emitted phonon energies from the sapphire substrate. Six dot lines labeled as line 1 to 6 connect similar dips in these FTIR spectra for different $Al_xGa_{1-x}N$ alloys. Due to the macroscopic electric field associated with the atomic displacements of the longitudinal optical phonons, the A_1 and E_1 optical modes are split into LO and TO components. Furthermore, as a result of the anisotropic nature of the wurtzite structure, these modes have an angular dependence. For phonon propagating along the c-axis, the A_1 mode is LO, while the two degenerate E_1 modes are TO. For the phonon propagating perpendicular to c-axis, the A_1 mode is transverse, while one of the E_1 modes is longitudinal and the other is transverse.[19] Since the samples were measured at a tilted angle, four phonon modes could be collected and analyzed. The dip positions were plotted in Fig. 4 with dependence of the Al composition. In general, the phonon frequencies increased with the aluminum composition can be observed in Fig. 3. The compositional dependence shown in the TO phonon energies were in agreement with the calculations based on ab initio interatomic force constants.[19] The blueshift of A_1 (TO) phonon with the increasing x can be primarily attributed to the decreasing reduced-mass in the unit cell. We also fitted the dip positions using linear functions except for the line 3 fitted by a quadratic functions and the results were listed in Table 1.

For the line 1, ω_0 = 545 cm^{-1} assigned as A_1 (TO) was in agreement with previous reports.[19-20, 21-23] This dashed line was fitted to respective data sets and $\omega_{A_1}(x) = 645 + 69 \cdot x$ [cm^{-1}]. The phonon frequencies along line 2 assigned as GaN like E_1 (TO) increased linearly with the Al compositions. However, dips became very broad when the Al composition was increased. The phonon frequencies along line 3 increased when Al composition was increased to 0.6 then deceased while the Al composition was increased further. These dips assigned as AlN like E_2 (TO) were also very broad. When in a pure AlN material, the two split peaks emerged into one broad peak. In an alloy, disorder breaks the symmetry of the modes and the q vector is no more strictly conserved, although it is still possible to have dispersion. Since the E_1 (TO) and E_2 (TO) in AlN are so flat and closed in energy, modes of different symmetry and q can mix together. As a result, from the linear extrapolation of experimental values for the GaN like E_1 (TO) phonon modes were $\varpi_{E_1}(x) = 608 + 46 \cdot x$ [cm^{-1}] and from the ploynominal extrapolation of experimental values for the AlN like E_2 (TO) phonon modes were $\varpi_{E_2}(x) = 628 + 158 \cdot x - 125 \cdot x^2$ [cm^{-1}]. Along line 4, the shallow dip positions increased slightly with the increase of Al composition. This mode was identified as the B_1 symmetry. Its frequency was linearly fitted as $\omega_{B_1}(x) = 692 + 29 \cdot x$ [cm^{-1}] in agreement with the previous reports.[19-20, 24] The silent B_1 mode manifested itself by an interference with an unidentified continuum.[22] The nonpolar B_1 mode did not depend on the phonon propagation direction. Its compositional and strain dependence was weak since the phonon frequency slope on the Al composition was small. Along line 5, the dips were not obvious because their frequencies were on the shoulder. We deduce the mode frequency

$\omega_{A_1}(x) = 765 + 84 \cdot x\,[\text{cm}^{-1}]$ from the linear extrapolation of experimental values. Along line 6, these dip frequencies are associated with the E_1 (LO) mode. From the linear extrapolation of experimental values, $\omega_{E_1}(\text{LO}) = 829 + 63x\,[\text{cm}^{-1}]$ could be obtained for the E_1 (LO) phonon modes. From the measurement results, we believe that FTIR reflectance measurements are sensitive to all these oscillating phonons. The A_1(TO) and E_1(LO) modes shall be the best candidates for the composition characterization of this system as they have small broadening and a pronounced dependence upon alloy composition.

A novel MOCVD growth process have been introduced in the active layer of UVLED. InGaN/AlGaN MQW with three pairs was grown by multi-step process and the schematic diagram of the growth procedure was shown in Figure 4. During growth of InGaN layer, thin InN layers were grown under various growth temperatures ranging from 650~685 ^{o}C and before AlGaN barrier growth, a growth interruption was introduced to treat the InN layer and make interdiffuse between InN and (Al)GaN layer to obtain InGaN layer. Figure 5 show the PL spectrum of sample with various InN growth temperatures. It shows that the blueshift of PL emission peak occurs as increase InN growth temperature. The sample whose InN layers were grown at 685 ^{o}C exhibited strong PL emission at 380 nm. Figure 6 shows the light-emitting pattern of the LED device. In order to realize the effect of growth temperature on PL peak shift and surface morphology modification, further microstructure analysis was required. The characterization of electroluminescence properties are in progress and the results of EL and detailed microstructure analysis will be presented in future report.

CONCLUSIONS

In conclusion, we reported a comprehensive study of the effects of composition on phonon modes in ternary $Al_xGa_{1-x}N$ grown on sapphire substrates using FTIR reflectance measurement. We obtained the composition dependence of the TO and LO phonons for each symmetry A_1 and E_1. The A_1 (TO), A_1 (LO) and E_1 (LO) phonons exhibited one-alloy mode behavior, while the E_1 (TO) phonons showed two-mode behavior. The silent B_1 mode was also observable due to partial or complete relaxation of selection rule in our samples. The A_1 (TO) and A_1 (LO) modes shall be good candidates for characterization of the alloy composition. The FTIR could become a non-destructive, convenient and even in-situ characterization tool for the AlGaN alloys.

InGaN/AlGaN MQW were grown by multi-step process. It was found that the PL spectra of the samples showed a strong UV emission at 380 nm. The growth temperature of InN dominates the PL emission peak position. The preliminary electroluminescence result was also shown. The InGaN/AlGaN MQW grown by multi-step process can be candidate to efficient UV LED.

.

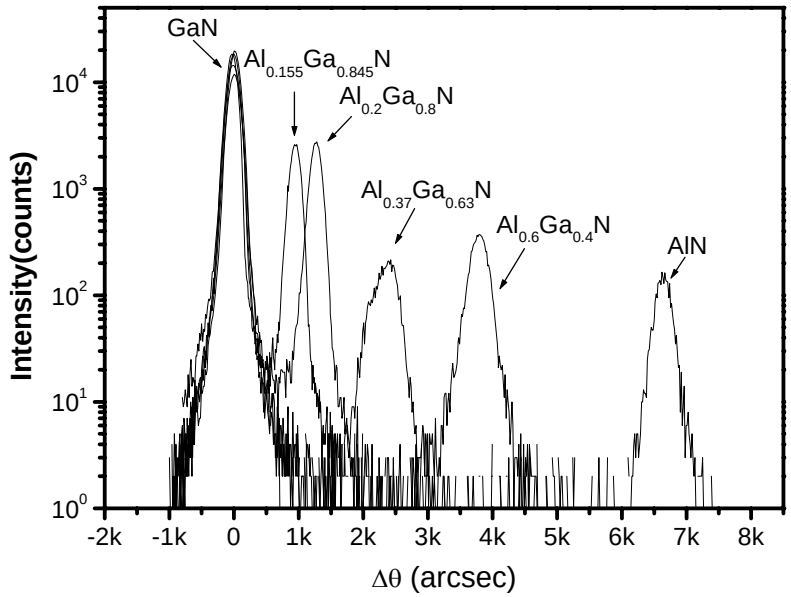

Fig. 1 x-ray double crystal rocking curve (0004) of $Al_xGa_{1-x}N$ samples grown on GaN/sapphire substrate.

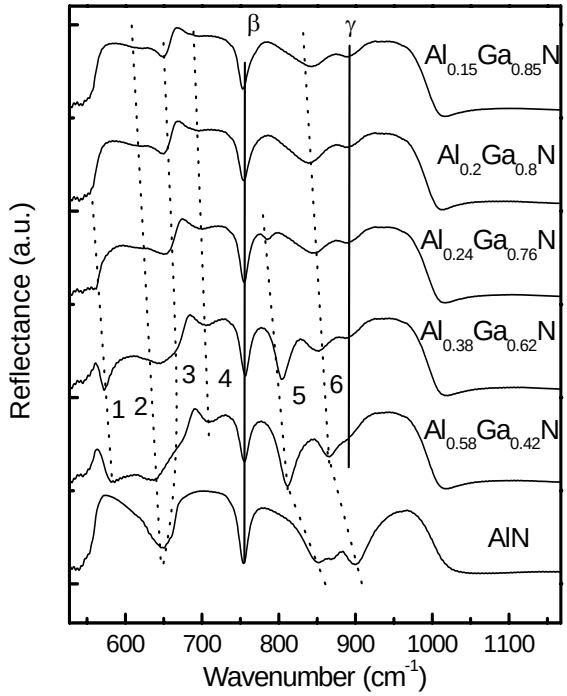

Fig. 2 FTIR reflectance spectra of different Al composition of AlGaN epilayer grown on sapphire.

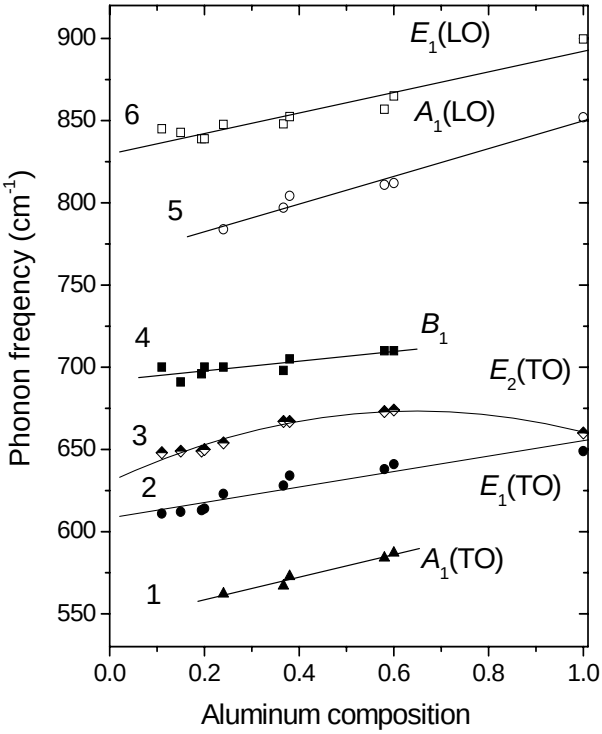

Fig. 3 Phonon energies versus composition x. the scatting symbols are from FTIR reflectance spectra, the solid lines are fits to respective data sets and results are listed in Table 1.

TABLE 1. Fit results for the phonon branches shown in Figs. 3. The fits were quadratic for the E_2(TO) band using $\omega(x) = \omega_0 + \alpha x + \beta x^2$. The data for the other phonons support only linear fits.

Line	Phonon branch and symmetry	ω_0 (cm^{-1})	α (cm^{-1})	β (cm^{-1})
1	A_1(TO)	545±3	69±7	--
2	GaN like E_1(TO)	608±3	46±6	--
3	AlN like E_2(TO)	628±4	158±15	-125±12
4	B_1	692±3	29±7	--
5	A_1(LO)	765±4	84±8	--
6	E_1(LO)	829±3	63±7	--

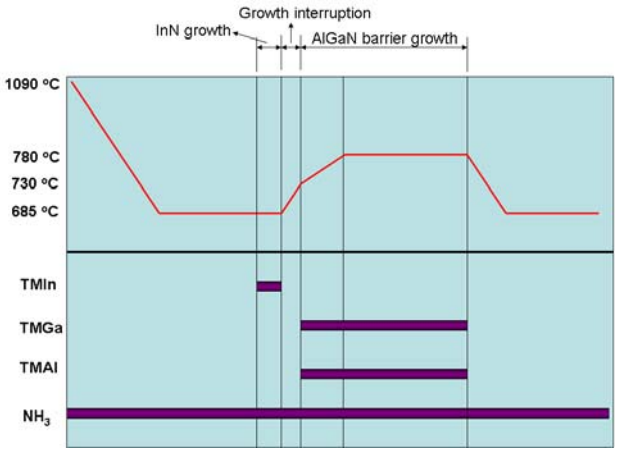

Fig. 4 The schematic diagram of multi-step growth procedure.

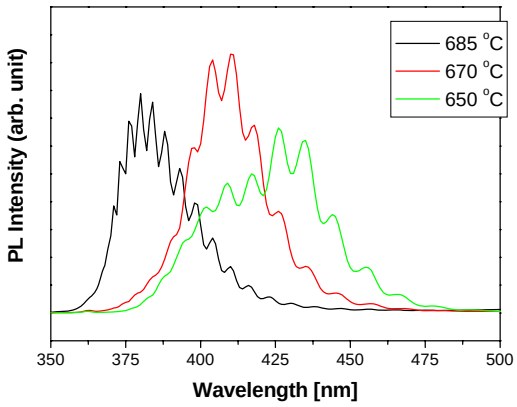

Fig. 5 PL spectra from the MQW grown at various InN growth temperature

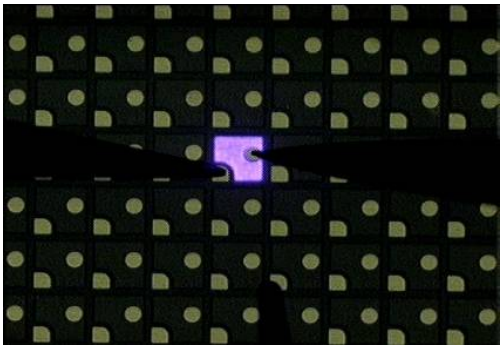

Fig. 6 The light-emitting pattern of the LED device.

References

[1] S. Nakamura, T. Mukai and M. Senou: Appl. Phys. Lett. **64** (1994) 1687.

[2] S. Nakamura, T. Mukai, M. Senoh and N. Iwasa: J. Appl. Phys. **76** (1994) 8189.

[3] S. Nakamura, M. Senoh, N. Iwasa, S. Nagahama, T. Yamada and T.Mukai: Jpn. J. Appl. Phys. **34** (1995) L1332.

[4] T. Mukai, D. Morita and S. Nakamura: J. Cryst. Growth **189/190** (1998) 778.

[5] T. Mukai, M. Yamada and S. Nakamura: Jpn. J. Appl. Phys. **37** (1998)L1358.

[6] T. Mukai, H. Narimatsu and S. Nakamura: Jpn. J. Appl. Phys. **37** (1998)L479.

[7] Y. Narukawa, I. Niki, K. Izuno, M. Yamada, Y. Murazaki and T. Mukai: Jpn. J. Appl. Phys. **41** (2002) L371.

[8] M. Iwaya, S. Terao, T. Sano, T. Ukai, R. Nakamura, S. Kamiyama, H. Amano and I. Akasaki: J. Cryst. Growth **237/239** (2002) 951.

[9] Y. B. Lee, T. Wang, Y. H. Liu, J. P. Ao, Y. Izumi, Y. Lacroix, H. D. Li, J. Bai, Y. Naoi and S. Sakai: Jpn. J. Appl. Phys. **41** (2002) 4450.

[10] T. Nishida, H. Saito and N. Kobayashi: Appl. Phys. Lett. **79** (2001) 711.

[11] A. Yasan, R. McClintock, K. Mayes, S. R. Darvish, H. Zhang, P. Kung, M. Razeghi, S. K. Lee and J. Y. Han: Appl. Phys. Lett. **81** (2002) 2151.

[12] T. Nishida, H. Saito and N. Kobayashi: Appl. Phys. Lett. **78** (2001) 399.

[13] T. Nishida, H. Saito and N.Kobayashi: Appl.Phys. Lett. **78** (2001) 3927.

[14] D. Morita, M. Yamamoto, K. Akaishi, K. Matoba, K. Yasutomo, Y. Kasai, M. Sano, S. Nagahama, T. Mukai, J. J. Appl. Phys. **43** (2004) 5945.

[15] H. Hirayama, J. Appl. Phys. **97** (2005) 091101.

[16] T. G. Kim, K. C. Kim, D. H. Kim, S. H. Yoon, J. W. Lee, C. S. Sone, Y. J. Park, J. Crystal Growth **272** (2004) 264.

[17] S. Y. Kwon, S. I, Baik, Y. W. Kim, H. J. Kim, D. S. Ko, E. Yoon, Appl. Phys. Lett. **86** (2005) 192105.

[18] G. S. Huang, T. C. Lu, H. H. Yao, H. C. Kuo, S. C. Wang, J. Appl. Phys. In press.

[19] C. Bungaro, S. D. Gironcoli, Appl. Phys. Lett. **76,** 2101 (2000).

[20] H. Grille and Ch. Schnittler Phys. Rev. B **61,** 6091 (2000).

[21] P. Wisniewski, W. Knap, J. P. Malzac, J. Camassel, M. D. Bremser, R. F. Davis, T. Suski, Appl. Phys. Lett. **73**, 1760 (1998).

[22] F. Demangeot, J. Frandon, M. A. Renucci, O. Briot, S. Clur, and R, L. Aulombard, Appl. Phys. Lett. **72**, 2674 (1998).

[23] M. Holtz, T. Prokofyeva, M. Seon, K. Copeland, J. Vanbuskirk, S. Williams, S. A. Nikishin, V. Tretyakov, H. Temkin, Appl. Phys. Lett. **89**, 7977 (2001).

[24] C. Bungaro, K. Rapcewicz, J. Berhole, Phys. Rev. B. **61,** 6720 (2000).

該計畫已有論文發表如下:

[1] G.S. Huang, H. H. Yao, T. C. Lu, H.C. Kuo, and S. C. Wang, “Aluminum incorporation into AlGaN grown by low-pressure metalorganic vapor phase epitaxy”, J. Appl. Phys., V99, 104901, (24 May, 2006)

[2] Y. J. Lee, J.M.Hwang, T. C. Hsu, M. H. Hsieh, M. J. Jou, B. J. Lee, T.C. Lu, H.C. Kuo, and S.C. Wang, “Enhancing Output Power of GaN-based LEDs Grown on Chemical Wet Etching Patterned Sapphire Substrate”, Photon. Tech. Lett., V18, No.10, pp1152-1155, (May, 2006)

[3] Te-Chung Wang, Hao-Chung Kuo, Tien-Chang Lu, Ching-En Tsai, Min-Ying Tsai, Jung-Tsung Hsu, Jer-Ren Yang, “Study of InGaN multiple Quantum Dots by MOCVD”, Jpn. J. Appl. Phys., Vol. 45, No. 4B, pp. 3560-3563 (April, 25, 2006)

[4] Hung-Wen Huang, Jung-Tang Chu, Chih-Chiang Kao, Tao-Hung Hsueh, Tien-Chang Lu, Hao-Chung Kuo, and Shing-Chung Wang, “Enhanced Light Output in InGaN/GaN Light Emitting Diodes with Excimer Laser Etching surfaces”, Jpn. J. Appl. Phys., Vol. 45, No. 4B, pp. 3442-3445, (April, 25, 2006)

[5] Y. J. Lee, J.M.Hwang, T. C. Hsu, M. H. Hsieh, M. J. Jou, B. J. Lee, T.C. Lu, H.C. Kuo, and S.C. Wang, “GaN-based LEDs with Al-Deposited V-Shape Sapphire Facet Mirror”, Photon. Tech. Lett, V18, No.5, pp724-726, (March, 2006)

[6] Yi-An Chang, Sheng-Horng Yen, Te-Chung Wang, Hao-Chung Kuo .,Yen-Kuang Kuo, Tien-Chang Lu, and Shing-Chung Wang “Experimental and Theoretical Analysis on Ultraviolet 370-nm AlGaInN Light-Emitting Diodes”, Semicon. Sci. Tech., V21, pp598-603 (21 March, 2006)

[7] H. H. Yao, T. C. Lu, G. S. Huang, C. Y. Chen, W. D. Liang, H. C. Kuo and S. C. Wang, “InGaN self-assembled quantum dots grown by metalorganic chemical-vapor deposition with interruption growth”, NanoTechnology, V17, pp1713-1716, (27 Feb 2006)

[8] G.S. Huang, T. C. Lu, H. H. Yao, H.C. Kuo, S. C. Wang, Chih-wei Lin and Li Chang “Crack-free GaN/AlN distributed Bragg reflectors incorporated with GaN/AlN superlattices grown by metal-organic chemical vapor deposition”, Appl. Phys. Lett., V88, 061904, (Feb, 2006)

[9] Y. J. Lee, T.C. Lu, H.C. Kuo, S.C. Wang, M. J. Liou, C.W. Chang, T. C. Hsu, M. H. Hsieh, M. J. Jou, and B. J. Lee, “High Brightness AlGaInP-based Light Emitting Diodes with the Stripe Patterned Omni-Directional Reflector”, Semicon. Sci. Tech., V11, pp1-6, (Feb, 2006)

[10] Y. J. Lee, T.C. Lu, H.C. Kuo, S.C. Wang, M. J. Liou, C.W. Chang, T. C. Hsu, M. H. Hsieh, M. J. Jou, and B. J. Lee, “AlGaInP LEDs with Stripe Patterned Omni-Directional Reflector”, Jpn. J. Appl. Phys., V45(2A), pp643-645, (Feb, 2006)

[11] Te-Chung Wang, Hao-Chung Kuo, Zheng-Hong Lee, Chang-Cheng Chuo, Min-Ying Tsai, Ching-En Tsai, Tsin-Dong Lee, Tien-Chang Lu, Jim Chi, “Quaternary AlInGaN multiple quantum well 368nm light-emitting diode”, J. Crystal Growth, V287 pp582-585, (Jan, 2006)

[12] Jung-Tang Chu, Chih-Chiang Kao, Hung-Wen Huang, Wen-Deng Liang, Chen-Fu Chu, Tien-Chang Lu, Hao-Chung Kuo and S.C. Wang, “Effects of different n-electrode patterns on optical characteristics of large-area p-side down InGaN light-emitting diodes fabricated by laser lift-off”, Jpn. J. Appl. Phys. V44, No.11, pp7910-7912, (2005)

本計畫期中報告結果自評

本計畫第一年已達成高鋁 AlGaN 的之磊晶技術與 InGaN 量子點磊晶技術，並成功以 InN 主動層的方式製作出 UV LED。同時發表多篇論文於 SCI 期刊上，並開發出傅氏變換紅外光譜在原位量測氮化鋁鎵的鋁成分和薄膜之厚度之技術，可充分展開第二年的研究進度包括將雷射剝離技術整合，可提升 UV LED 的操作效率。

附件二

可供推廣之研發成果資料表

☐ 可申請專利　■ 可技術移轉　　日期：95 年 5 月 25 日

國科會補助計畫	計畫名稱：藍紫光發光元件磊晶及製程之研究(1/3) 計畫主持人：王興宗 教授 計畫編號：NSC 94－2215－E009－082　學門領域：
技術/創作名稱	傅氏變換紅外光譜在原位量測氮化鋁鎵的鋁成分和薄膜之厚度
發明人/創作人	黃根生，盧庭昌，姚忻宏，郭浩中，王興宗
技術說明	中文：利用有機金屬氣相磊晶系統成長不同鋁成分氮化鋁鎵薄膜。光學聲子 A_1 (TO)，E_1 (TO)，A_1 (LO) 和 E_1 (LO)的頻率隨鋁成分而改變。A_1 (TO) 和 A_1 (LO) 光學聲子呈現單模並有良好的對稱性，窄的線寬以及對鋁成分的大的線型變化。A_1 (TO) 和 A_1 (LO) 光學聲子隨鋁成分線型變化的斜率分別為 69 和 84 cm^{-1}。這些光學聲子將是決定氮鋁鎵的鋁成分和結構的最好的參數。另外，膜的厚度由兩邊的干涉峰算出。傅氏變換紅外光譜在原位量測其氮化鋁鎵的鋁成分及膜的厚度。
	英文：High quality $Al_xGa_{1-x}N$ (0<x<1) alloys grown by MOCVD were studied by using X-ray diffraction and Fourier transform infrared reflectance (FTIR) measurements. The Al compositional dependence of phonons having A_1 (TO), E_1 (TO), A_1 (LO) and E_1 (LO) symmetry was determined. The A_1 (TO) and A_1 (LO) modes, displayed a one-mode behavior and had a well defined symmetry, small linewidth and a large linear dependence of the phonon frequency upon alloy composition. The A_1 (TO) and A_1 (LO) modes linearly increased with Al composition by the large slopes of 69 and 84 cm^{-1}, respectively. In additional, the film thickness increase with interference fringes on both sides. These phonons modes shall be the best candidates for the compositional and structural characterization of AlGaN alloys.
可利用之產業及可開發之產品	可用於紫外光發光二極體和高電子遷移率的電晶體的產業。 可開發出傅氏變換紅外光譜原位測量儀。
技術特點	簡單、無損傷和非接觸式的原位量測。在磊晶成長和製程過程皆可應用。
推廣及運用的價值	開發出傅氏變換紅外光譜原位測量儀可廣泛應用於光電產業。一方面，提升光電產業的量測品質;另一方面，開發的量測機台可推出市場。

※ 1. 每項研發成果請填寫一式二份，一份隨成果報告送繳本會，一份送　貴單位研發成果推廣單位（如技術移轉中心）。

※ **2. 本項研發成果若尚未申請專利，請勿揭露可申請專利之主要內容。**

※ 3. 本表若不敷使用，請自行影印使用。